Optimal Beam Matching in Particle Accelerators via Extremum Seeking

Eugenio Schuster, Eiji Morinaga, Christopher K. Allen and Miroslav Krstić

***Abstract*— The matching problem for a low energy transport system in a charged particle accelerator is approached using the extremum seeking feedback method for non-model based optimization. The beam dynamics are modeled using the KV (Kapchinsky-Vladimirsky) envelope equations. Extremum seeking is employed for the lens tuning in the beam matching system. Numerical simulations illustrate the effectiveness of this approach.**

I. Introduction

In a particle accelerator, charged particles such as electrons, protons, or heavy ions are accelerated by electromagnetic fields to serve as light source (e.g., synchrotron radiation) or to collide with targets. In the last case, as a result of the collision many other subatomic particles are created and detected. From the information collected by the detectors, properties of the particles and their interactions can be determined. Accelerators are used for research in high-energy and nuclear physics, synchrotron radiation, medical therapies, and some industrial applications. The higher the energy of the accelerated particles, the more closely the structure of matter can be probed.

The first stage of the particle accelerator is the source. In this stage, charged particles are produced, either ions via an ion source, or electrons via a cathode. Particle accelerators come in two basic designs: linear (linac) and circular (synchrotron). The longer the main section of the linac, the higher the energy of the particles it can produce. The length of a linac can be on the order of kilometers, and more. In both the linac and the synchrotron, the particles gain energy by interacting with electromagnetic fields. For a traveling wave structure, bunches of ions are accelerated in the same way a surfer is pushed along by a wave. This is achieved by synchronizing the passage of the particles with the phase of the accelerating field. Standing wave structures, and static field machines, use RF gaps instead to accelerate the particles. At the end of the main section the high-energy beam of charged particles hits the target.

In the design of a particle accelerator, feedback control systems are becoming an essential part of the system. The uses of control are numerous: from the magnet power supplies, to RF systems, to various control loops dedicated to certain properties of the beam (steering, phase and position in storage rings, etc.). In this work we approach the beam matching problem, where the beam must be matched to the acceptance ellipse of an accelerating structure or transport section. Specifically we consider a fixed geometry matching section consisting of four quadrupole lenses. The objective of this system is to take any arbitrary initial beam state and "match" it to the acceptance ellipse of the following section, i.e., any given initial state x_{ini} to a prescribed final state x_{fin}, through the control of the lens strengths in the transport (matching) channel. A review of beam transport including matching was recently presented in [1]. We assume the matching channel to be composed of discrete beamline elements, such as lenses, and drifts. These elements are cascaded along the beam axis, considered the z axis, to form the matching channel. This configuration is depicted in Figure 1. The input to the lenses, labeled θ_1, θ_2, θ_3, and θ_4 in the figure, represent the focusing strength of the lenses and are the parameters of the channel that may be varied.

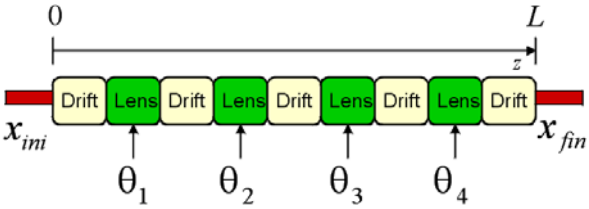

Fig. 1. Matching Channel

The optimal control of the lens strengths to match a beam from an initial state to a prescribed final state was already approached by one of the authors [2] for the six lenses case, an under-determined situation, using local (nonlinear programming) and global (dynamic programming) methods. The global method is practical only for axisymmetric systems. It has been shown to become too computationally intensive for particle beams with more degrees of freedom. For these beams, the local method is substantially faster at the expense of finding local minima of the cost functional, which may not be the best (global) solution. The major shortcoming of these methods is their dependence on the model. The accuracy of the calculation is limited by the uncertainties associated with the initial beam conditions, magnet modeling, exact beam current, emittances, magnet locations, etc. Therefore, the implementation of the calculated element strengths in a real experiment does not yield true matching conditions. Under these circuntances, the "knobs" for the lens strengths must be adjusted on-line. The success of such a procedure relies at

E. Schuster is with the Department of Mechanical Engineering and Mechanics, Lehigh University, 19 Memorial Drive West, Bethlehem, PA 18015-0385, USA, schuster@lehigh.edu

E. Morinaga is with the Department of Computer-Controlled Mechanical Systems, Osaka University, 2-1 Yamadaoka, Suita, Osaka 565-0871, Japan, morinaga@newton.mech.eng.osaka-u.ac.jp

C.K. Allen is with Los Alamos National Laboratory, Los Alamos, NM 87545, USA, ckallen@lanl.gov

M. Krstić is with the Department of Mechanical and Aerospace Engineering, University of California at San Diego, 9500 Gilman Dr., La Jolla, CA 92093-0411, USA, krstic@ucsd.edu

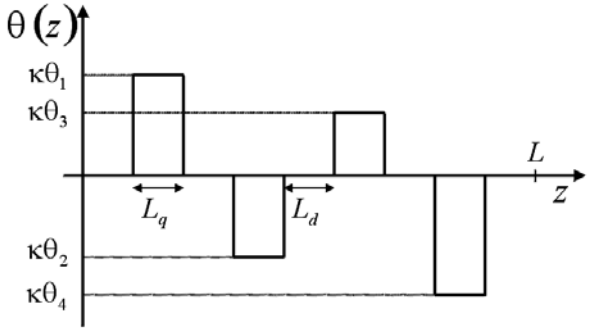

Fig. 2. Focusing function

present completely upon the experience, judgement, and intuition of the operator. In this work we consider the usage of extremum seeking as optimization technique. As a real-time non-model-based optimization technique, extremum seeking is well suited to overcome the limitations described above for model-based optimization methods. The performance of this technique in terms of robustness against uncertainties, computational demand, and ability to deal with cost functions full of local minima, is reported.

The paper is organized as follows. In Section 2 the optimization problem is defined. Section 3 introduces the fundamentals of extremum seeking. The results of the simulation study are presented in Section 4. The paper is closed by a summary in Section 5.

II. Problem Definition

Assuming a continuous, elliptically-symmetric particle beam, we model its dynamics using the KV coupled-envelope equations [3]. Let the z coordinate represent the position along the design trajectory, and thus the xy plane is the transverse plane for the particle beam. At each z location, let $X(z)$ and $Y(z)$ represent the semi-axes of the beam envelope in the x and y planes, respectively. The KV equations then appear as

$$X'' - \theta(z)X - \frac{2K}{X+Y} - \frac{\epsilon_X^2}{X^3} = 0 \quad (1)$$

$$Y'' + \theta(z)Y - \frac{2K}{X+Y} - \frac{\epsilon_Y^2}{Y^3} = 0 \quad (2)$$

where the prime indicates differentiation with respect to z, that varies from 0 to L and plays the role of "time". The function $\theta(z)$ is the focusing (control) function. K is the beam perveance, ϵ_X and ϵ_Y are the effective emittances of the beam in the x and y planes, respectively. The focusing function $\theta(z)$, is shown in Figure 2; κ is a constant, L_d is the drift length, and L_q is the quadropole lens length. The matching channel parameters (lens strengths) must satisfy the following constraints: $0 \leq \theta_1, \theta_3 \leq 50$, and $-50 \leq \theta_2, \theta_4 \leq 0$.

We are given initial conditions for the beam at $z = 0$, the transport system's entrance location. These conditions characterize the beam coming from the preceding section of the transport or accelerator system. They may be translated into initial conditions for the beam envelopes in the x plane (X_{ini}, X'_{ini}) and in the y plane (Y_{ini}, Y'_{ini}). In matching systems we are also given desired final conditions, or target conditions, at $z = L$, the exit location of the matching channel. We denote this target conditions as (X_{tar}, X'_{tar}) and (Y_{tar}, Y'_{tar}). They are prescribed by the acceptance requirements of the next section of the transport or accelerator system.

Denoting $x = [X \quad X' \quad Y \quad Y']^T$, we define

$$x_{ini} = x(0) = \begin{bmatrix} X_{ini} \\ X'_{ini} \\ Y_{ini} \\ Y'_{ini} \end{bmatrix}, \; x_{fin} = x(L) = \begin{bmatrix} X_{fin} \\ X'_{fin} \\ Y_{fin} \\ Y'_{fin} \end{bmatrix}. \quad (3)$$

In addition, we define a target value for x denoted as $x_{tar} = [X_{tar} \quad X'_{tar} \quad Y_{tar} \quad Y'_{tar}]^T$, and desired beam profiles (beam trajectories) for $X(z)$ and $Y(z)$ denoted as $X_{des}(z)$ and $Y_{des}(z)$ respectively. Given x_{ini}, x_{tar}, $X_{des}(z)$ and $Y_{des}(z)$, we use an extremum seeking procedure to minimize the cost function J given by

$$\begin{aligned} J &= \{k_1 J_1 + k_2 J_2 + k_3 J_3\}^{\frac{1}{2}} \quad (4) \\ J_1 &= K_X \left(X_{fin} - X_{target}\right)^2 + K_Y \left(Y_{fin} - Y_{target}\right)^2 \\ J_2 &= K_{dX} \left(X'_{fin} - X'_{target}\right)^2 + K_{dY} \left(Y'_{fin} - Y'_{target}\right)^2 \\ J_3 &= \int_0^L w(z) \Big[K_{iX} \left(X(z) - X_{des}(z)\right)^2 \\ &\quad + K_{iY} \left(Y(z) - Y_{des}(z)\right)^2\Big] dz, \end{aligned}$$

where K_X, K_Y, K_{dX}, K_{dY}, K_{iX}, and K_{iY} are weight constants, and w_z is an integral weight function.

The problem is formulated as finite-"time" optimal control ($0 \leq z \leq L$), with bang-bang controls of fixed durations but varying intensities (i.e., with a very coarse discretization in "time" which results in a highly constrained waveform for the control θ as it is shown in Fig. 2), for a plant that is nonlinear. This is far from being a standard optimization problem. To add complexity to the problem, we are seeking robustness against uncertainties of the system for a successful practical implementation of the control method.

III. Extremum Seeking

Extremum seeking control, a popular tool in control applications in the 1940-50's, has seen a resurgence in popularity as a real time optimization tool in different fields of engineering [4]. Extremum seeking is applicable in situations where there is a nonlinearity in the control problem, and the nonlinearity has a local minimum or a maximum. The parameter space can be multivariable. In this paper we use extremum seeking for iterative optimization of θ to make x_{fin} as close as we can to x_{tar}. For each new value of θ we run the KV equations and obtain x_{fin}. We point out that, since x_{tar} is given arbitrarily, x_{fin} is obtained via solving a system of nonlinear differential equations, and the lens input applied through θ is highly constrained in its waveform, there may not exist θ such that perfect matching is achieved, $x_{fin} = x_{tar}$, thus we try to obtain the best possible *approximate* matching. We change θ after each beam "run." Thus, we employ the discrete time variant [5] of extremum seeking. The implementation is depicted in Figure 3, where q

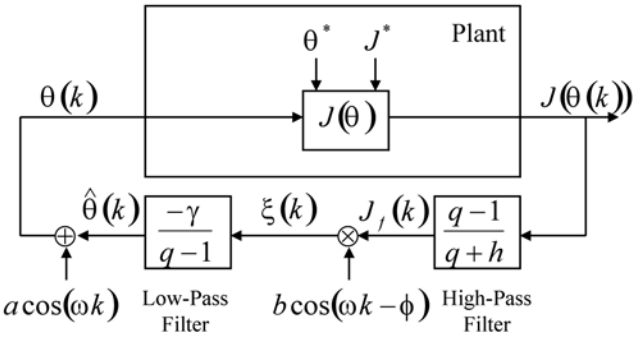

Fig. 3. Extremum seeking control scheme

denotes the variable of the Z-transform. The high-pass filter is designed as $0 < h < 1$, and the modulation frequency ω is selected such that $\omega = \alpha\pi$, $0 < |\alpha| < 1$, and α is rational. The static nonlinear block $J(\theta)$ corresponds to one run of the KV system. The objective is to minimize J. If J has a global minimum its value is denoted by J^* and its argument by θ^*.

In this case, we are dealing with a multi-parameter extremum seeking procedure, where the variables are written as

$$\theta(k) = \begin{bmatrix} \theta_1(k) \\ \theta_2(k) \\ \theta_3(k) \\ \theta_4(k) \end{bmatrix}, \hat{\theta}(k) = \begin{bmatrix} \hat{\theta}_1(k) \\ \hat{\theta}_2(k) \\ \hat{\theta}_3(k) \\ \hat{\theta}_4(k) \end{bmatrix}, \xi(k) = \begin{bmatrix} \xi_1(k) \\ \xi_2(k) \\ \xi_3(k) \\ \xi_4(k) \end{bmatrix}.$$

The extremum seeking constants shown in Figure 3 are written as $a = b = diag(\begin{bmatrix} a_1 & a_2 & a_3 & a_4 \end{bmatrix})$, and $\gamma = diag(\begin{bmatrix} \gamma_1 & \gamma_2 & \gamma_3 & \gamma_4 \end{bmatrix})$. In addition, we denote

$$\cos(\omega k) = \begin{bmatrix} \cos(\omega_1 k) \\ \cos(\omega_2 k) \\ \cos(\omega_3 k) \\ \cos(\omega_4 k) \end{bmatrix}, \cos(\omega k - \phi) = \begin{bmatrix} \cos(\omega_1 k - \phi_1) \\ \cos(\omega_2 k - \phi_2) \\ \cos(\omega_3 k - \phi_3) \\ \cos(\omega_4 k - \phi_4) \end{bmatrix}.$$

In each iteration of the extremum seeking procedure, $\theta(k)$ is used to compute the focusing function $\theta(z)$, shown in Figure 2, which is in turn fed into the KV equations (1) and (2). Given x_{ini}, the KV equations are integrated to obtain $X(z)$, $Y(z)$, and x_{fin}. The output of the nonlinear static map, $J(k) = J(\theta(k))$, is then obtained by evaluating (4) and used to compute $\theta(k+1)$ according to the extremum seeking procedure in Figure 3, or written equivalently as

$$\begin{aligned} J_f(k) &= -hJ_f(k-1) + J(k) - J(k-1) && (5) \\ \xi(k) &= J_f(k) b \cos(\omega k - \phi) && (6) \\ \hat{\theta}(k+1) &= \hat{\theta}(k) - \gamma\xi(k) && (7) \\ \theta(k+1) &= \hat{\theta}(k+1) + a\cos(\omega(k+1)). && (8) \end{aligned}$$

IV. Simulation Results

The physical parameters used in the simulations presented in this section are $K = 2.7932 \times 10^{-6}$, $\epsilon_X = 6 \times 10^{-6}$, $\epsilon_Y = 6 \times 10^{-6}$, $\kappa = 2.6689$, $L_d = 0.1488$, $L_q = 0.0610$, and $L = 0.988$. In addition, the extremum seeking parameters are $h = 0.4$, $\omega_i = \omega_{base}^i \times \pi$, $\gamma_i = 0.1\frac{M(\omega_1)}{M(\omega_i)}$, and $\phi_i = -\phi(\omega_i)$ for $i = 1, \ldots, 4$, where $\omega_{base} = 0.95$, and $M(\omega)$ and $\phi(\omega)$ are respectively the magnitude and phase of the frequency response of the high-pass filter in Figure 3.

For all the simulations, the initial condition of the beam at the entrance of the channel and the target condition are

$$x_{ini} = \begin{bmatrix} 0.001474 \\ -0.006013 \\ 0.002014 \\ 0.007686 \end{bmatrix}, x_{tar} = \begin{bmatrix} 0.001094 \\ -0.007865 \\ 0.003290 \\ 0.011726 \end{bmatrix}, \quad (9)$$

and the initial conditions for the extremum seeking parameters are $\theta_1(0) = \theta_3(0) = 25$, and $\theta_2(0) = \theta_4(0) = -25$.

Terminal Constraints Only: Figures 4 and 5 show the extremum seeking results when the cost function parameters are given by

$$\begin{aligned} &K_X = 2000,\ K_Y = 1000,\ K_{dX} = 0,\ K_{dY} = 0, \\ &K_{iX} = K_{iY} = 0,\ k_1 = 1,\ k_2 = 0,\ k_3 = 0. \end{aligned} \quad (10)$$

The converged value of θ, and its associated final state, are

$$\hat{\theta}_{fin} = \begin{bmatrix} 28.0635 \\ -33.4561 \\ 23.7620 \\ -34.4235 \end{bmatrix}, x_{fin} = \begin{bmatrix} 0.001091 \\ -0.007151 \\ 0.003294 \\ 0.007128 \end{bmatrix}. \quad (11)$$

Comparing x_{fin} with x_{tar}, we can note that we have a very good matching for X and Y, which was our goal ($k_2 = k_3 = 0$). However, although the matching for X' is probably acceptable, the matching for Y' is not. Figure 4-c shows the beam envelope as a function of z for $\theta = \hat{\theta}_{fin}$. The time evolution of θ_1, θ_2, θ_3, θ_4 in Figure 4- b shows a fast convergence. We can see that after 100 iteration we arrive to what we can consider a steady state situation. This fast convergence can be also noted looking at the evolution of the cost function in Figure 4-a. The complexity of the problem is evident from Figure 5 where the cost function is plotted as a function of θ_1, θ_2, θ_3, θ_4. Each combination of θ's defines a case. In Figure 5-a, θ_i, for $i = 1, 2, 3, 4$, is varied from 0 to 50 in steps of 5. In Figure 5-b, θ_i, for $i = 1, 2, 3, 4$, is varied from 35 to 41 in steps of 1. The negative peak corresponds to $\theta = \begin{bmatrix} 38 & -38 & 38 & -38 \end{bmatrix}^T$, which seems to be a global minimum. In Figure 5-c, θ_1 is varied from 27.8 to 28.3, θ_2 is varied from -33.2 to -33.7, θ_3 is varied from 23.5 to 24, θ_4 is varied from -34.2 to -34.7 in steps of 0.1. This figure shows that $\hat{\theta}_{fin}$ in (11) is a local minimum.

In order to obtain a better matching for the derivatives, we considered the case characterized by the cost function parameters

$$\begin{aligned} &K_X = 2000,\ K_Y = 1000,\ K_{dX} = 1,\ K_{dY} = 1, \\ &K_{iX} = K_{iY} = 0,\ k_1 = 1,\ k_2 = 1,\ k_3 = 0. \end{aligned} \quad (12)$$

Figures 6 shows the extremum seeking results. The converged value of θ, and its associated final state, are

$$\hat{\theta}_{fin} = \begin{bmatrix} 35.978 \\ -33.933 \\ 21.384 \\ -32.508 \end{bmatrix}, x_{fin} = \begin{bmatrix} 0.001070 \\ -0.006730 \\ 0.003289 \\ 0.011034 \end{bmatrix}. \quad (13)$$

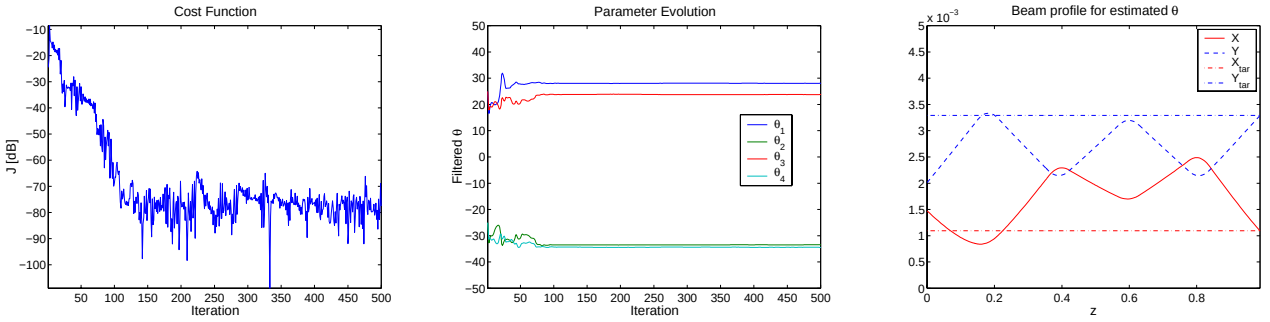

(a) (b) (c)

Fig. 4. Cost function evolution (a), θ evolution (b), beam profile for θ_{fin} (c)

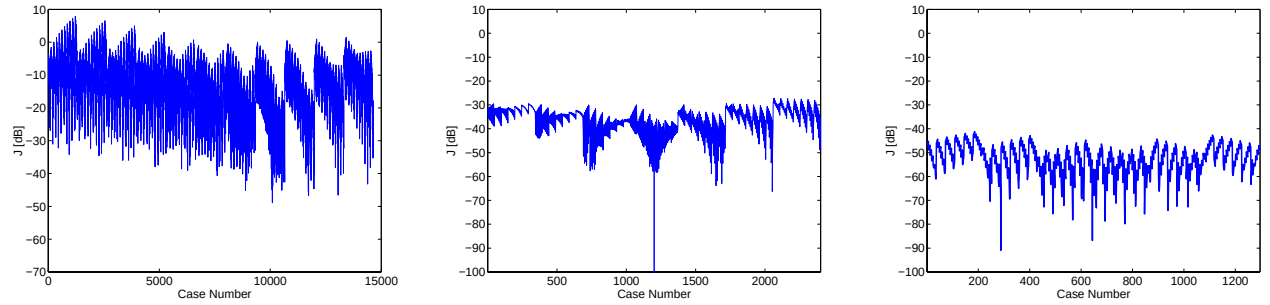

(a) (b) (c)

Fig. 5. Cost function map for different combinations of θ_1, θ_2, θ_3, θ_4

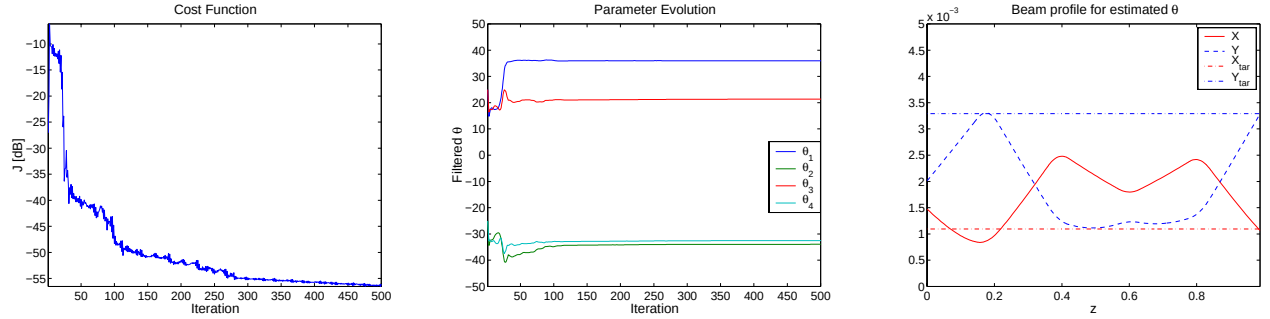

(a) (b) (c)

Fig. 6. Cost function evolution (a), θ evolution (b), beam profile for θ_{fin} (c)

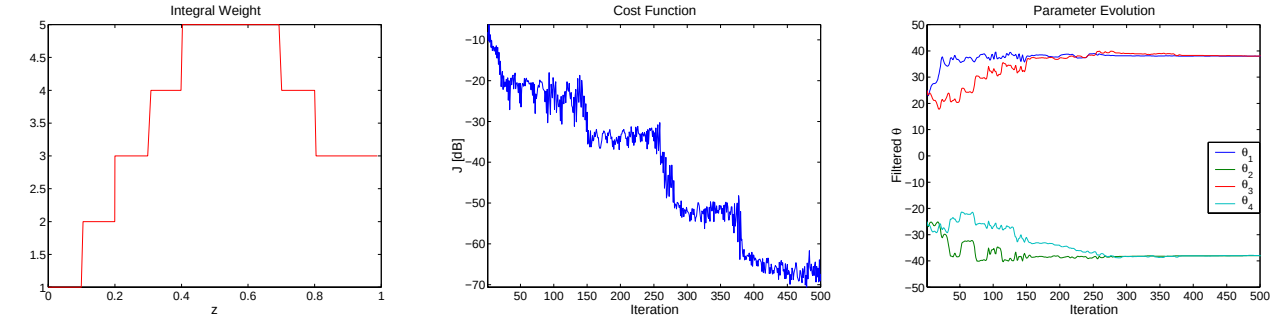

(a) (b) (c)

Fig. 7. Integral weight (a), cost function (b), θ evolution (c)

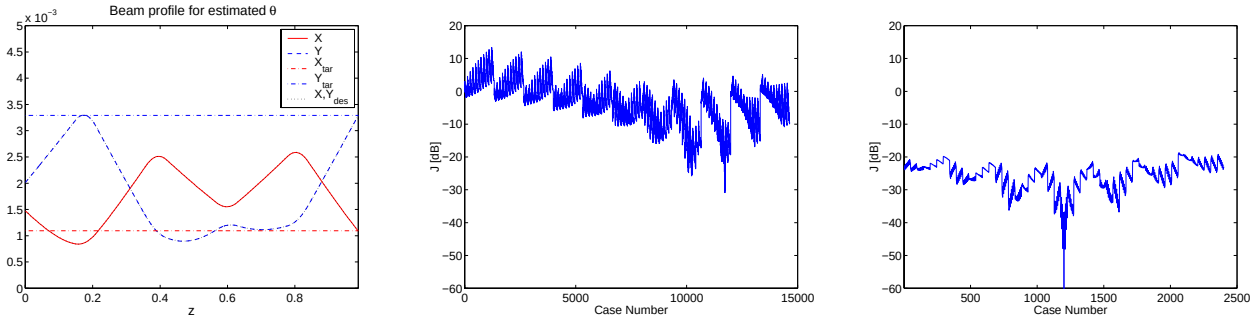

(a) (b) (c)

Fig. 8. Beam profile for θ_{fin} (a). Cost function map for different combinations of θ_1, θ_2, θ_3, θ_4 (b), (c).

Comparing x_{fin} with x_{tar}, we can note that we still have a very good matching for X and Y, and we improve the matching for Y' keeping an acceptable matching for X'. It is interesting to note that the value for $\hat{\theta}_{fin}$ is very different from the one in the previous case. Figure 6-c shows the beam envelope as a function of z for $\theta = \hat{\theta}_{fin}$. The time evolution of θ_1, θ_2, θ_3, θ_4 in Figure 6-b shows that the convergence is not as fast as in the previous case, where we only care for the matching of X and Y, but it is indeed very good. We can see that after 200 iteration we arrive to an acceptable solution which improves even more with subsequent iterations. This can be also noted from Figure 6-a, where the cost function does not reach a steady value after 500 iterations. This is an indication that the result can be improved by increasing the number of iterations or possibly by changing some of the variables of the extremum seeking procedure.

Real Trajectory as Desired Trajectory: We are interested in determining whether the extremum seeking procedure could converge to the global minimum if more information about this minimum were given. In this case we take $X_{des}(z)$ and $Y_{des}(z)$ as the solution of the KV equations when $\theta = [\ 38 \quad -38 \quad 38 \quad -38\ ]^T$, the global minimum. The cost function parameters are chosen as

$$\begin{aligned} &K_X = 200,\ K_Y = 200,\ K_{dX} = 1,\ K_{dY} = 1, \\ &K_{iX} = K_{iY} = 10000,\ k_1 = 1,\ k_2 = 1,\ k_3 = 1, \end{aligned} \tag{14}$$

and the weight $w(z)$ is chosen as shown in Figures 7-a. Figures 7 and 8 show the extremum seeking results. The converged value of θ, and its associated final state, are

$$\hat{\theta}_{fin} = \begin{bmatrix} 38.028 \\ -38.025 \\ 38.123 \\ -38.011 \end{bmatrix},\ x_{fin} = \begin{bmatrix} 0.001095 \\ -0.007871 \\ 0.003291 \\ 0.011725 \end{bmatrix}. \tag{15}$$

Comparing x_{fin} with x_{tar}, we can note that we have an acceptable matching. In this case we are indeed converging to $\theta = [\ 38 \quad -38 \quad 38 \quad -38\ ]^T$, the global minimum. Figure 8-a shows the beam envelope as a function of z for $\theta = \hat{\theta}_{fin}$, where it is possible to note that X and Y perfectly match X_{des} and Y_{des} respectively. The time evolution of θ_1, θ_2, θ_3, θ_4 in Figure 7-c shows that a steady value is reached after less than 400 iterations. This can also be noted from the evolution of the cost function in Figure 8-b. This figure also shows the effect of varying a_1, a_2, a_3 and a_4 as functions of the value of J. It is possible to note the steps in the evolution of J thanks to the change of the sinusoidals' amplitudes. Figure 8 also shows the cost function plotted as a function of θ_1, θ_2, θ_3, θ_4. In Figure 8-b, θ_i, $i = 1, 2, 3, 4$ is varied from 0 to 50 in steps of 5. In Figure 8-c, θ_i, $i = 1, 2, 3, 4$ is varied from 35 to 41 in steps of 1. The negative peak for the case $\theta = [\ 38 \quad -38 \quad 38 \quad -38\ ]^T$ is manifested in this figure. Comparing this map with the ones corresponding to the cases with only terminal constrains we can note that the map is not as spiky and in average (after an imaginary low-pass filter) a better parabola is described.

Double Linear Interpolation as Desired Trajectory: The evolution of the beam profile corresponding to the global minimum is not available in real applications. The designer is therefore required to have an intuitive understanding as to what makes a good desired trajectory. The beam envelope will track the desired trajectory as closely as possible. These conditions leads to optimality only if the desired trajectory is chosen properly (in an optimal sense). The choice of the desired trajectory is particularly important for under-determined systems where the number of lenses is strictly higher than four. In these cases the solution for the matching problem (i.e., making $x_{fin} = x_{tar}$) is not unique and the choice of the desired trajectory has a decisive influence on the outcome of the optimization procedure. In this case we take $X_{des}(z)$ and $Y_{des}(z)$ as a combination of two linear functions as shown in Figure 10-a (dotted line). The slope of the last section of the desired beam profile coincides with the target conditions for the derivatives in order to facilitate their matching. The use of only one linear function, connecting X_{ini} and Y_{ini}, with X_{tar} and Y_{tar} respectively, would be in conflict with the terminal conditions for the derivatives. Figures 9 and 10 show the extremum seeking results when the cost function parameters are given by

$$\begin{aligned} &K_X = 2000,\ K_Y = 2000,\ K_{dX} = 1,\ K_{dY} = 1, \\ &K_{iX} = K_{iY} = 50,\ k_1 = 1,\ k_2 = 1,\ k_3 = 1. \end{aligned} \tag{16}$$

The integral weight $w(z)$ is shown in Figures 9-a. We try not only to match the final section of the beam profile but also to reduce excursions in the middle section. The converged

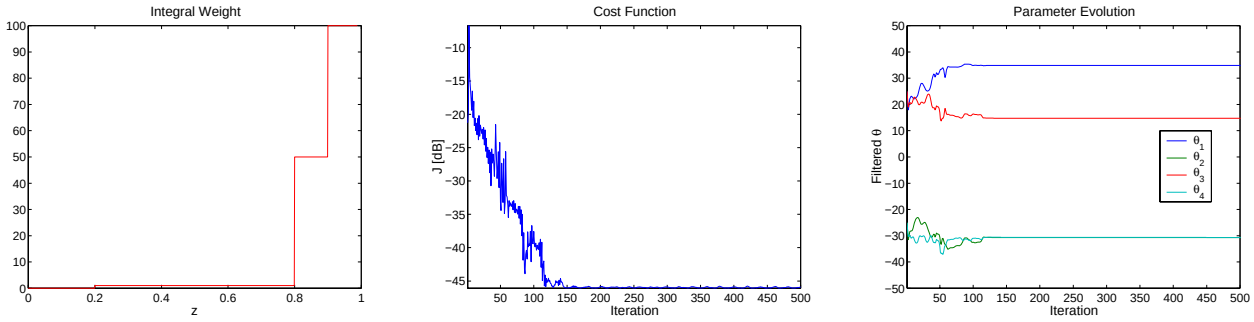

(a) (b) (c)

Fig. 9. Integral weight (a), cost function (b), θ evolution (c)

value of θ, and its associated final state, are

$$\hat{\theta}_{fin} = \begin{bmatrix} 34.855770 \\ -30.710796 \\ 14.736266 \\ -30.669086 \end{bmatrix}, x_{fin} = \begin{bmatrix} 0.001093 \\ -0.007343 \\ 0.003280 \\ 0.010630 \end{bmatrix}. \quad (17)$$

Comparing x_{ini} with x_{target}, we can note that we do have a very good matching for the final conditions. It is interesting to note how different is the value of $\hat{\theta}_{fin}$ from the global minimum and at the same time how good is the matching. The time evolution of θ_1, θ_2, θ_3, θ_4 in Figure 9-c shows that a steady value is reached after 150 iterations. This can be also noted from Figure 9-b, where the cost function does reach a steady value after 150 iterations, showing a very fast convergence. Figure 10 shows the beam profile for θ_{fin}. Not only the matching of the target conditions is very good, but also the matching of the desired profile. This is explained by how the cost function was defined. The figure also compares the beam profile for θ_{fin} with the nominal profile ($\theta = [\ 38 \quad -38 \quad 38 \quad -38\ ]^T$). From the comparison we can conclude that we achieve very similar final conditions reducing at the same time the excursion of $X(z)$ and $Y(z)$.

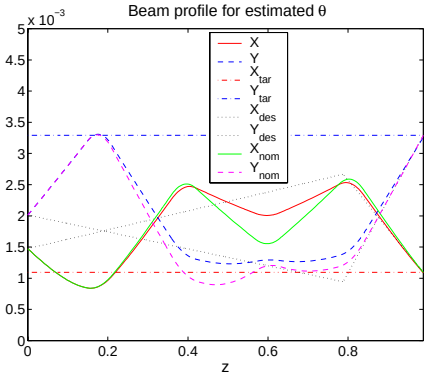

Fig. 10. Beam profile for θ_{fin}

V. Conclusions

A multi-parameter extremum seeking procedure has been implemented, and successfully tested in simulations, for the tuning of the lens strengths in a 4-lens matching channel. Based on the promising results obtained in the simulation study, it is anticipated that the scheme can play an important role in an off-line design process. In terms of convergence speed, the method compares to or outperforms previously proposed schemes based on nonlinear and dynamic programming. In terms of globality, the method resides between them. Although globality cannot be guaranteed, we must highlight at this point the capability of the scheme of avoiding getting stuck in local minima with relatively large values of the cost function. The modification of the amplitude of the sinusoidal excitation as a function of the value of the cost function is key in this achievement. Such modification is motivated by the expertise of the operator and his knowledge of the sensitivity of the beam size at the end of the matching channel with respect to the different lenses. This suggests the possibility of designing an extremum seeking scheme that automatically adapts their gains or sinusoidal amplitudes to permanently seek a lower value of the cost function. This potential scheme would be very useful for applications with spiky cost function maps as the one considered in this work.

In addition, the scheme can be used for real-time optimization taking advantage of its non-model-based nature, which represents an advantage with respect to other model-based optimization techniques such as nonlinear and dynamic programming. To accelerate convergence, a hybrid scheme is envisioned where the optimal lens strengths are computed off-line using extremum seeking or another optimization technique, and used as initial conditions ($\theta(0)$) for an on-line extremum seeking controller. Under this framework, the extremum seeking algorithm will be playing the role of a non-model-based adaptive controller, which is one of its unique characteristics, that ensures a well-matched beam at the end of the matching channel independently of the uncertainties in the system parameters.

References

[1] S.M. Lund and B. Bukh, "Stability properties of the transverse envelope equations describing intense ion beam transport," *Phys. Rev. ST Accelerators and Beams*, vol. 7, 024801, 2004.

[2] C.K. Allen and M. Reiser, "Optimal transport of particle beams," *Nuclear Instruments and Methods in Physics Research*, A 384, 1997, pp 322-332.

[3] I.M. Kapchinskij and V.V. Vladimirskij, *Proc. Int. Conf. on High-Energy Accelerators and Instrumentation*, CERN, 1959, pp. 274-288.

[4] K. Ariyur and M. Krstic, *Real-Time Optimization by Extremum Seeking Feedback*, Wiley, 2003.

[5] J.-Y. Choi, M. Krstic, K. Ariyur and J.S. Lee, "Extremum seeking control for discrete-time systems," *IEEE Transactions on Automatic Control*, vol. 47, no. 2, pp. 318-323, 2002.